

# 8λ×200 Gb/s WDM Transmission Enabled by a Hybrid-Integrated Comb Source Without Optical Amplification

Stefano Grillanda\*, Di Che, Cristian Bolle, Mark Cappuzzo, Rose Kopf

Nokia Bell Labs, Murray Hill, NJ 07974, United States, \*[stefano.grillanda@nokia-bell-labs.com](mailto:stefano.grillanda@nokia-bell-labs.com)

**Abstract** We demonstrate 8-channel WDM transmission with 200 Gb/s net bit-rate per wavelength enabled by a hybrid-integrated comb source with 6 dBm output power per channel and without optical amplification. We show unamplified transmission across 820 m of standard single mode fiber in the C-band. ©2023 The Author(s)

## Introduction

Short-reach optical systems, such as for datacenter interconnects and high-performance computing [1-2], can scale their capacity through architectures that use multiple wavelengths with coarse channel spacing and simple modulation formats (e.g., on-off keying or 4-level pulse amplitude modulation) instead of more complex coherent technologies [3]. These systems typically leverage arrays of compact, low-power and high-bandwidth electro-optic modulators, that can operate across broad wavelength bands, such as microring modulators [2], surface-normal electroabsorption modulators [4] or waveguide-based electroabsorption modulators [5].

Furthermore, these systems can benefit from the use of comb sources and multi-wavelength lasers, that can be used as central light sources [6] and that generate many wavelengths with a single integrated device [2,7-9]. These devices include, e.g., arrays of distributed feedback lasers combined with a multiplexer [2], quantum-dot comb lasers [7] and Kerr-frequency combs [8]. However, many of these approaches, such as Kerr frequency combs, have often low optical output power, and require additional optical amplifiers to have sufficient power for modulation and to meet the power budget of the system.

Here, we use a hybrid-integrated comb

source, that we recently demonstrated [9], with ~6 dBm optical power per wavelength, to enable an 8λ×200 Gb/s wavelength division multiplexing (WDM) system without optical amplification. The results align well with the emerging industrial demand of 1.6T transceivers which are expected to be in mass production in a few years [10]. Our comb source is made by hybrid integration of reflective semiconductor optical amplifiers (RSOAs) and a silica chip. We show transmission in the C-band across spans of standard single-mode fiber (SSMF) up to a length of 820 m (dispersion ~13.6 ps/nm). Our transmission results in the C-band can be potentially obtained as well in the O-band (with a much longer reach for the same dispersion tolerance), where many short-reach intensity-modulation direct detection systems operate, since our comb source approach can be re-designed for operation in different wavelength ranges.

## Hybrid-Integrated Comb Source

Figures 1(a-b) show a photograph and a circuit schematic of our hybrid-integrated comb source, made of 16 III-V based RSOAs integrated with a passive silica chip. The RSOAs have high-reflectivity (HR) back facets, which form the first mirror of the comb laser, and anti-reflection coatings on the front facets. The silica chip hosts

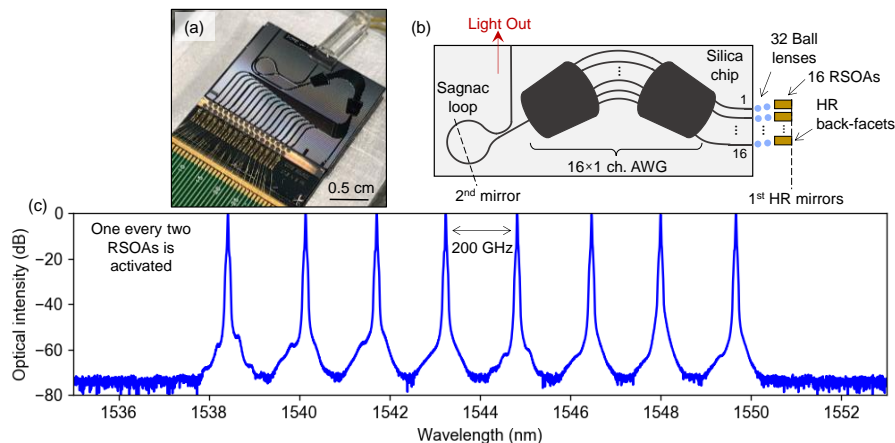


**Fig. 1:** (a) Photograph and (b) schematic of the hybrid-integrated comb source. (c) Output spectrum when 8 RSOAs are activated (one every two): the output has 8 channels with 200 GHz spacing, each channel has ~6 dBm optical power.

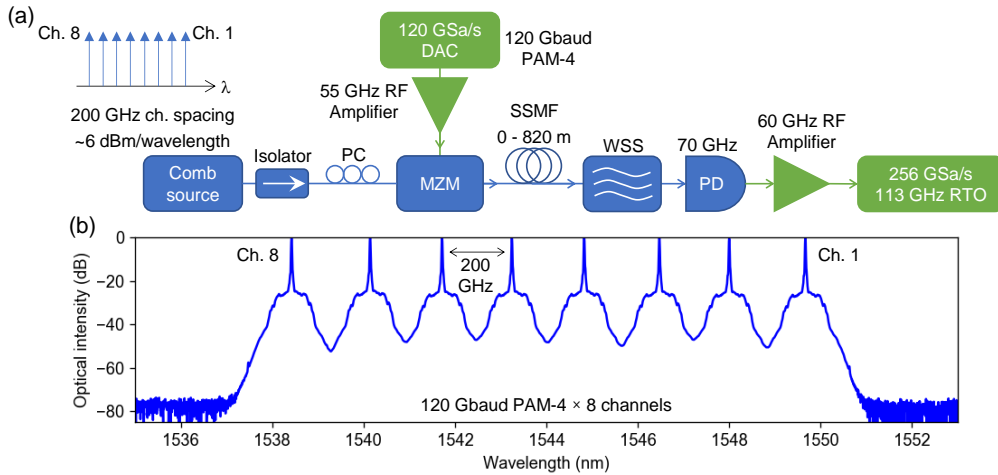


**Fig. 2:** (a) Setup used in the transmission experiments with the hybrid-integrated comb source. (b) Optical spectrum of the  $8 \times 120$  Gbaud PAM-4 WDM signal measured after the MZM. Channels are numbered from long to short wavelengths.

a  $16 \times 1$  channel arrayed waveguide grating (AWG) with 100 GHz channel spacing and a Sagnac loop, that behaves as the second, partial-reflectivity, mirror of the comb laser. Each RSOA is coupled to one of the 16 input waveguides of the AWG by a pair of ball lenses (32 in total). The AWG passbands select a narrow band from the RSOAs broadband spectrum. On increasing the RSOAs currents, lasing on each channel occurs when the roundtrip gain is higher than the roundtrip cavity loss. Also, the AWG combines the light of each RSOA on the same output waveguide and its channel spacing determines the spacing between the comb wavelengths.

The comb source of Figs. 1(a-b) can emit 16 wavelengths spaced by 100 GHz; however, in this work we target 8 channels with 200 GHz spacing, and since each channel can be activated independently from the others, we turn on one every two RSOAs. Also, we optimize the RSOAs currents to equalize the output power of the channels [minimum current for channels 2 and 7 (130 mA) and maximum for channel 1 (210 mA)]. As shown in Fig. 1(c), the output spectrum of the comb source is made of 8 continuous-wave (CW) wavelengths, spaced by 200 GHz; each wavelength has  $\sim 6$  dBm optical output power (with a difference between highest and lowest power channels of  $\sim 0.4$  dB). The linewidth of the channels is on the order of few kHz [9].

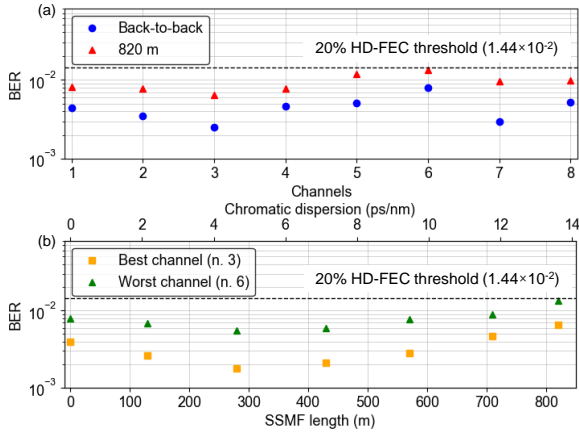
### Transmission Experiments

Figure 2(a) shows the setup for the transmission experiments. CW light at the comb source output is sent to a lithium niobate Mach-Zehnder modulator (MZM) with 35 GHz bandwidth and smooth frequency response decay. The total optical power at the comb source output is  $\sim 15$  dBm (*i.e.*,  $\sim 6$  dBm/ $\lambda$ ). An isolator at the comb source output minimizes optical reflections and a polarization controller (PC) optimizes the

polarization at the MZM input. We bias the MZM at the quadrature point and drive it with a 120 Gbaud PAM-4 electrical signal generated by a 120 GSa/s digital-to-analog-converter (DAC) sampling at one sample per symbol. A radio-frequency (RF) amplifier with 55 GHz frequency response and 23 dB gain increases the DAC signal before application to the MZM. Linear pre-equalization is performed to compensate for the frequency response roll-off from both the DAC and the modulator. Figure 2(b) shows the optical spectrum of the 8-channel WDM signal after the MZM. Channels are numbered from long to short wavelengths. The total optical signal power at the MZM output is  $\sim 7.1$  dBm.

We investigated transmission performance of the channels up to 820 m of SSMF (dispersion  $\sim 16.6$  ps/nm/km). The accumulated dispersion of  $\sim 13.6$  ps/nm after 820 m corresponds to about 7 km SSMF transmission at 1330 nm. The receiver is composed by a wavelength selective switch (WSS) with 200 GHz passband that selects the channel under test from the comb of transmitted channels. Then, the channel under test is detected with a 70 GHz photodetector (PD) and a 256 GSa/s real-time oscilloscope (RTO) with 113 GHz electrical bandwidth. Due to the lack of a transimpedance amplifier in the PD, an RF amplifier with 60 GHz bandwidth and 22 dB gain is used to increase the PD output signal to match the RTO sensitivity. No optical amplification is used in our experiments.

To measure the bit-error-ratio (BER) of the channels we perform offline digital signal processing (DSP) at the receiver. Our DSP includes timing recovery, a 400-tap feed forward equalization (FFE) at 2 samples per symbol (sps), a maximum likelihood sequence estimation (MLSE) at 1 sps with 1-tap memory (*i.e.*, 16 states for PAM-4 signals), and the symbol decision. Figure 3(a) shows the BER of the



**Fig. 3:** (a) BER of the channels in back-to-back and after 820 m of SSMF. (b) BER of the best and worst channels versus transmission length and dispersion. To achieve different transmission lengths, we cascaded several SSMF spools (6 in total for 820 m length); the total additional optical loss of the spools including connectors is  $\sim 0.8$  dB for 820 m with respect to the back-to-back case.

channels in back-to-back and after 820 m of SSMF: the BER of all channels is under the threshold of the hard-decision (HD) forward error correction (FEC) with 20% overhead ( $1.44 \times 10^{-2}$ ) [11] in both cases. The net bit-rate per channel is 200 Gb/s. Channel 3 has best BER and channel 6 has the worst: differences from channel to channel primarily come from differences in optical power at the PD which, in back-to-back, range from  $-5.3$  dBm for the best channel (n. 3) to  $-6.2$  dBm for the worst channel (n. 6). Besides  $\sim 0.4$  dB power difference between best and worst CW comb tones, the remaining power variation mainly comes from the WSS. Also, the penalty after 820 m with respect to back-to-back is mostly due to the lower power at the PD in this case. In fact, the 820 m length was obtained by cascading several SSMF spools (6 in total) of shorter lengths with 0.8 dB total additional loss (including connectors) compared to the back-to-back case.

In Fig. 3(b) we show the BER of the best and worst channels versus propagation distance across SSMF and dispersion. As shown by the BER of the worst channel, transmission is under the 20% HD-FEC level up to 820 m of SSMF (dispersion  $\sim 13.6$  ps/nm) for all channels, with best BER after about 280 m of SSMF (dispersion  $\sim 4.6$  ps/nm). In our system with no optical amplification, the BER after fiber transmission is impacted by the interaction of the fiber dispersion with the residual chirp of the MZM, and by the additional optical loss of the fiber spools.

### Power Budget Discussion

Since our system is limited by the receiver sensitivity, the BER and the margin available can be further improved by increasing the output power of the comb source channels. Figure 4(a)

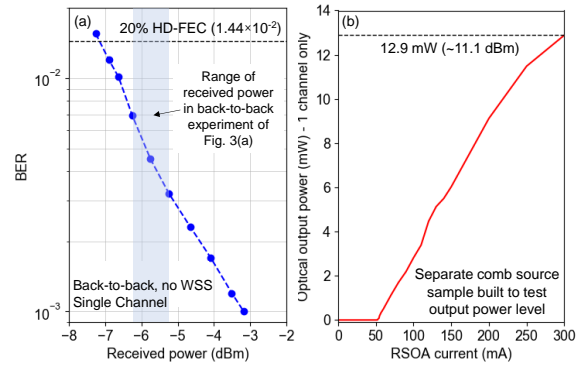


**Fig. 4:** (a) Receiver sensitivity of the 120-Gbaud PAM-4 signal in back-to-back with only one channel active and without WSS before the PD. (b) Output power of one channel of a separate comb source built to show the power improvement that can be obtained with our design.

shows the receiver sensitivity measured in back-to-back with only one comb source channel active and without the WSS before the PD. A 3 dB improvement in the output power of the comb source channels would provide 3 dB higher power at the PD and, according to Fig. 4(a), would improve the back-to-back BER of the worst channel, that is  $8 \times 10^{-3}$  with  $-6.2$  dBm optical power at the PD [Fig. 3(a), channel 6], to  $10^{-3}$ .

Indeed, our comb source design allows to obtain higher output power than the  $\sim 6$  dBm/ $\lambda$  used in this work. As discussed in [9], to sustain higher power when many comb source channels are active, a better cooling of the RSOAs and thermal isolation is needed. To prove the potential power improvement, we built a separate comb source sample, with same design as in Figs. 1(a-b) but where we assembled only one RSOA (*i.e.*, one active channel). In this sample, we measured the optical output power versus RSOA current [Fig. 4(b)]: the power can be increased to  $\sim 12.9$  mW (11.1 dBm) at 300 mA, which represents a 5 dB improvement compared to the comb source prototype used in this work. Finally, this potential 5 dB improvement in output power of the comb source channels may provide additional margin needed in a real WDM system where a demultiplexer and multiplexer would be used at the transmitter to separate the comb source channels and then recombine them again after being modulated by an array of modulators.

### Conclusions

We demonstrated  $8\lambda \times 200$  Gb/s WDM transmission without optical amplification using a hybrid-integrated comb source with  $\sim 6$  dBm optical output power per channel.

### Acknowledgements

We thank the Nokia Advanced Optics Group for providing the RSOAs used in the comb source, B. Farah and G. Raybon for help with the setup.

## References

- [1] S. Fatholouloumi, D. Hui, S. Jadhav, J. Chen, K. Nguyen, M. N. Sakib, Z. Li, H. Mahalingam, S. Amiralizadeh, N. N. Tang, H. Potluri, M. Montazeri, H. Frish, R. A. Defrees, C. Seibert, A. Krichevsky, J. K. Doylend, J. Heck, R. Venables, A. Dahal, A. Awujoola, A. Vardapetyan, G. Kaur, M. Cen, V. Kulkarni, S. S. Islam, R. L. Spreitzer, S. Garag, A. C. Alduino, RK Chiou, L. Kamyab, S. Gupta, B. Xie, R. S. Appleton, S. Hollingsworth, S. McCargar, Y. Akulova, K. M. Brown, R. Jones, D. Zhu, T. Liljeberg, and L. Liao, "1.6 Tbps Silicon Photonics Integrated Circuit and 800 Gbps Photonic Engine for Switch Co-Packaging Demonstration," *Journal of Lightwave Technology* vol. 39, no. 4, pp. 1155-1161, Feb. 2021.  
DOI: <https://doi.org/10.1109/JLT.2020.3039218>
- [2] M. Wade, E. Anderson, S. Ardalani, W. Bae, B. Beheshtian, S. Buchbinder, K. Chang, P. Chao, H. Eachempatti, J. Frey, E. Jan, A. Katzin, A. Khilo, D. Kita, U. Krishnamoorthy, C. Li, H. Lu, F. Luna, C. Madden, L. Okada, M. Patel, C. Ramamurthy, M. Raval, R. Roucka, K. Robberson, M. Rust, D. Van Orden, R. Zeng, M. Zhang, V. Stojanovic, F. Sedgwick, R. Meade, N. Chan, J. Fini, B. Kim, S. Liu, C. Zhang, D. Jeong, P. Bhargava, M. Sysak, and C. Sun, "An Error-free 1 Tbps WDM Optical I/O Chiplet and Multi-wavelength Multi-port Laser," *Proceedings of the Optical Fiber Communications Conference 2021*, art no. F3C.6.  
DOI: <https://doi.org/10.1364/OFC.2021.F3C.6>
- [3] M. Sysak, J. Johnson, D. B. Lewis, and C. Cole, "CW-WDM MSA technical specifications," 2021. [Online]. Available: <https://cw-wdm.org>
- [4] S. Grillanda, C. Tran, D. Che, T.-C. Hu, N. Basavanahally, R. Papazian, R. Kopf, A. Tate, M. Cappuzzo, M. Earnshaw, K. W. Kim, G. Raybon, D. Neilson, and P. Iannone, "4x53 Gbit/s Electro-Optic Engine with a Surface-Normal Electroabsorption Modulator Array," *IEEE Photonics Technology Letters*, vol. 35, no. 8, pp. 426-429, Apr. 2023.  
DOI: <https://doi.org/10.1109/LPT.2023.3254479>
- [5] J. S. Levy, E. Timurdogan, Y.-S. Kuo, G. Y. Lyu, C. Tsai, X. Yan, H. Kim, C. Stagarescu, K. Meneou, A. Thomas, I. Fragkos, G. Sitwell, A. Trita, Y. Liu, M. Ziebel, J. Byrd, S. Steinbach, B. Chou, W. Vis, A. Abed, Y. Kwon, H. Nykanen, S.-H. Lo, J. Ikonen, J. Larismaa, J. Drake, A. Benzoni, C. Minkenberg, T. Schrans, and A. Rickman, "4x100Gb/s PAM4 Multi-Channel Silicon Photonic Chipset with Hybrid Integration of III-V DFB Lasers and Electro-Absorption Modulators," *Journal of Lightwave Technology*, pp. 1-10, Mar. 2023.  
DOI: <https://doi.org/10.1109/JLT.2023.3263069>
- [6] B. Buscaino, E. Chen, J. W. Stewart, T. Pham, and J. M. Kahn, "External vs. integrated light sources for intra-data center co-packaged optical interfaces," *Journal of Lightwave Technology*, vol. 39, no. 7, pp. 1984-1996, Apr. 2021.  
DOI: <https://doi.org/10.1109/JLT.2020.3043653>
- [7] G. Kurczveil, X. Xiao, A. Descos, S. Srinivasan, L. Di, and R. G. Beausoleil, "High-temperature error-free operation in a heterogeneous silicon quantum dot comb laser," *2022 Optical Fiber Communications Conference and Exhibition (OFC)*, San Diego, CA, USA, 2022, pp. 1-3.  
DOI: <https://doi.org/10.1364/OFC.2022.Tu2E.2>
- [8] A. Rizzo, A. Novick, V. Gopal. B. Y. Kim, X. Ji, S. Daudlin, Y. Okawachi, Q. Cheng, M. Lipson, A. L. Gaeta, and K. Bergman, "Integrated Kerr frequency comb-driven silicon photonic transmitter," arXiv:2109.10297 (2021). [Online] Available: <https://arxiv.org/abs/2109.10297>
- [9] S. Grillanda, C. Bolle, M. Cappuzzo, R. Papazian, B. Farah, F. Pardo, P. Iannone, N. Fontaine, M. Mazur, R. Kopf, and M. Earnshaw, "Hybrid-Integrated Comb Source With 16 Wavelengths," *J. Lightwave Technol.* vol. 40, no. 21, pp. 7129-7135, Nov. 2022.  
DOI: <https://doi.org/10.1109/JLT.2022.3198022>
- [10] T. Rahman, Md. S. Hossain, N. Stojanovic, S. Calabrò, J. Wei, C. Xie, and M. Kuschnerov, "1.6Tb/s Transmission Feasibility Employing IM/DD for Datacentre Networks," *2020 European Conference on Optical Communications (ECOC)*, Brussels, Belgium, 2020, pp. 1-4,  
DOI: <https://doi.org/10.1109/ECOC48923.2020.9333418>
- [11] L. M. Zhang and F. R. Kschischang, "Staircase Codes With 6% to 33% Overhead," *Journal of Lightwave Technology*, vol. 32, no. 10, pp. 1999-2002 May 2014.  
DOI: <https://doi.org/10.1109/JLT.2014.2316732>